7. Chain orientation

7.1. Introduction

Chain orientation is a phenomenon unique to polymers. The uni-dimensional nature of the linear polymer chain makes it possible to obtain strongly anisotropic properties. The anisotropy arises when molecules are aligned along a common director (Fig. 7.1). The intrinsic properties of a polymer chain are strongly directionally dependent. The strong covalent bonds along the chain axis and the much weaker secondary bonds in the transverse directions cause a significant anisotropy of any given tensor property (**x**) (Fig. 7.1). The concept of orientation would be meaningless if the chain-intrinsic properties were isotropic

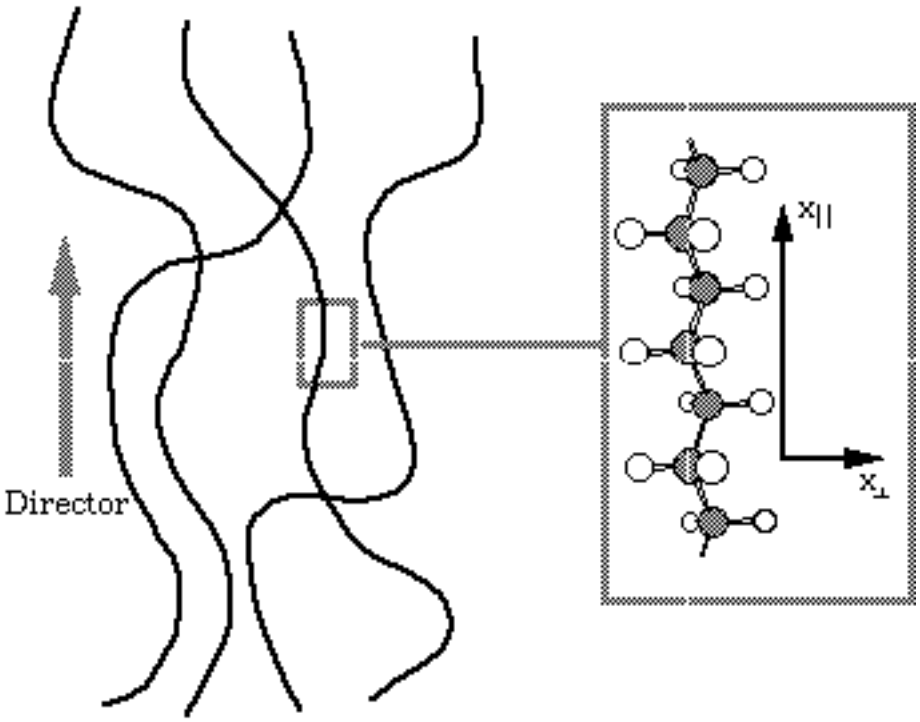

Fig. 7.1. Schematic illustration of the concept of chain orientation. The average preferential direction (director) is shown. The insert figure illustrates the intrinsic anisotropy of a polymer chain.

Chain orientation refers always to a particular structural unit (Fig. 7.2). It may be a whole sample or a macroscopic part of a specimen. The core of an injection-moulded specimen is typically unoriented, whereas the material of the same specimen closer to the surface is oriented. The director varies as a function of location in both types of

sample, which points to the fact that it is possible to find smaller ‘domains’ of higher degree of orientation (Fig. 7.2). In semi-crystalline polymers, the crystalline and amorphous components show different degrees of orientation.

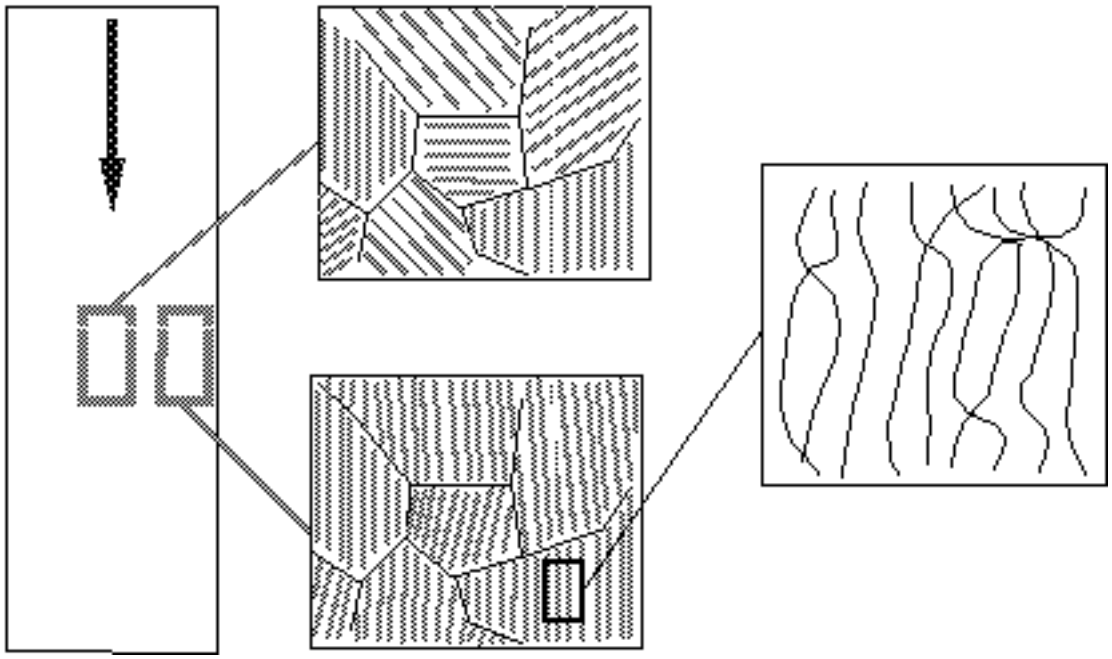

Fig. 7.2. Chain orientation in relation to sample size showing the orientation at two different locations in the cross-section of an injection-moulded sample (left-hand part, arrow indicates flow direction). The middle sample is unoriented, whereas the surface sample is highly oriented along the flow direction.

Quiescent polymeric melts with a size of millimetres or larger essentially never show global orientation. It is well known that liquid crystalline polymers show local orientation. However, if a molten polymer is subjected to external forces of mechanical, electric or magnetic origin, the molecules may align along a common director. The oriented state is however only temporary and prevails only under the influence of the external field. If the orienting field is removed, the molecules relax to adopt a random orientation. The rate at which the oriented system approaches the unoriented state depends on the molecular architecture (primarily molar mass), the order of liquid (e.g. the presence of liquid crystallinity) and the monomeric frictional coefficient (see chapter 6 for a detailed discussion). Very rapid solidification of an oriented melt makes it possible to make permanent the chain orientation. Rapid solidification can be

achieved by rapid cooling at constant pressure or by rapid elevation of the hydrostatic pressure at constant temperature.

7.2. Definition of chain orientation

7.2.1. General background

Chain orientation should not be confused with mechanical strains or frozen-in deformations. Orientation is the result of deformation but a given strain may result in very different degrees of orientation as the following example illustrates. The average square end-to-end distance of a random coil molecule is given by:

$$\left\langle r^2 \right\rangle_0 = Cnl^2 \tag{7.1}$$

where C is the characteristic ratio that depends on the segmental flexibility, l is the bond length and n is the number of bonds. A fully oriented molecule has the end-to-end distance:

$$r_\infty = l\cos\alpha \;\; n \tag{7.2}$$

where α is the angle between the chain axis and the individual bonds of the extended chain. The strain (λ) necessary to reach the completely extended state is given by:

$$\lambda = \frac{r_\infty}{\left(\left\langle r^2 \right\rangle_0\right)^{1/2}} = \frac{\cos\alpha\sqrt{n}}{\sqrt{C}} \tag{7.3}$$

The strain to reach full extension, i.e. to attain complete orientation thus increases with the square root of the molar mass. There is thus no unique relationship between degree of orientation and strain.

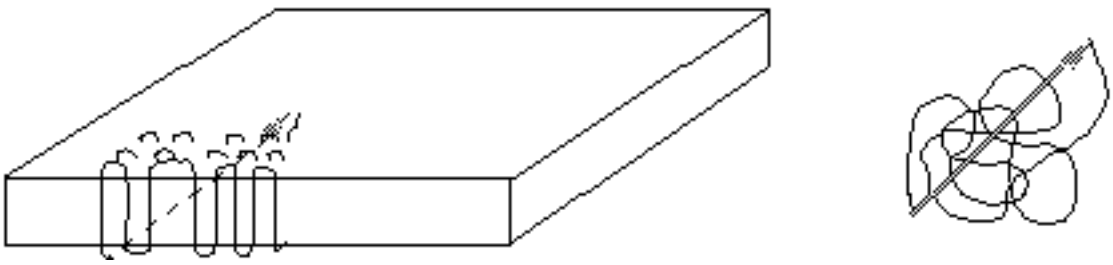

Fig. 7.3. A chain in a single crystal and a Gaussian chain.

Fig. 7.3 illustrates the possible lack of correlation between segmental orientation and the degree of extension of the end-to-end vector. The orientation of the segments of a molecule in the single crystal is indeed very high. More than 90% of the molecule is perfectly aligned provided that the crystal thickness is greater than 10 nm. The end-to-end vector is not, however, very extended. The Gaussian chain shows a similar end-to-end group separation but the segmental orientation is completely random. Segmental orientation is revealed by measurement of optical birefringence, wide-angle X-ray diffraction and infrared spectroscopy. Neutron scattering has assessed the orientation of the end-to-end vector. Furthermore, it has been noticed that the stiffness of ultra-oriented fibres does not correlate with Hermans orientation function but instead with the draw ratio which more sensitively reflects the extension of the end-to-end vector. Hence, some properties depend strongly on segmental orientation whereas other properties are more controlled by the end-to-end vector orientation.

7.2.2. The Hermans orientation function

The Hermans orientation function (f) is probably the quantity most frequently used to characterize the orientation. This orientation function was derived by the Dutch scientist P. H. Hermans in 1946 and is part of an equation, which relates optical birefringence to segmental orientation. A brief derivation is presented here. The first assumption made is that the polarizability associated with each chain segment can be described by a component parallel to the chain axis (p_1) and a component perpendicular (p_2) to the same chain axis (Fig. 7.4). The orientation of the chain segment with respect to coordinate system is schematically shown in Fig. 7.4. It is assumed that the electrical vector of the propagating light is along the **z**-axis. The electrical field parallel to the chain axis is $E_z \cos \phi$ and the polarization along the chain segment is given by $p_1 E_z \cos \phi$, The contribution of this polarization to the polarization along the **z** axis amounts to $p_1 E_z \cos^2 \phi$.

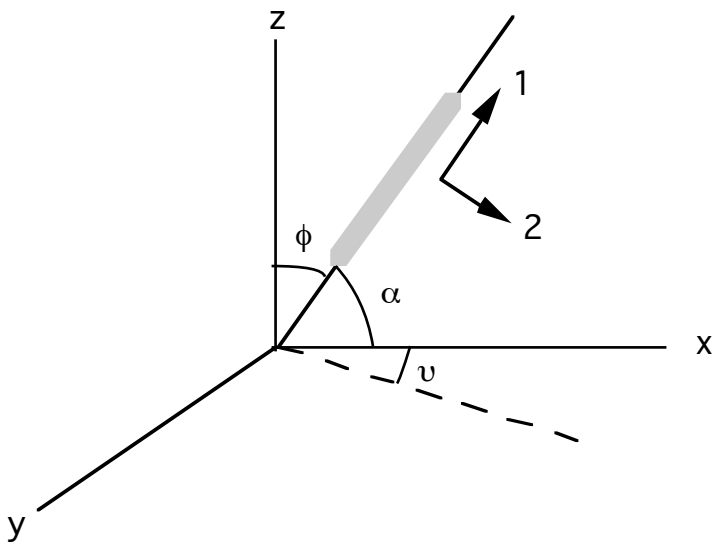

Fig. 7.4. Chain segment and coordinate system

§The contribution to polarization along **z** from the transverse polarization of the segment (i.e. along vector 2; Fig. 7.4) is by analogy equal to $E_z\ p_2\ \sin^2\phi$. The total polarization along the **z**-axis caused by the electrical vector in the z direction (P_{zz}) is equal to the sum of these two contributions:

$$P_{zz} = E_z\left(p_1\cos^2\phi + p_2\sin^2\phi\right) \tag{7.4}$$

The polarizability in the **z** direction (p_{zz}) is given by:

$$p_{zz} = \frac{P_{zz}}{E_z} = p_1\cos^2\phi + p_2\sin^2\phi \tag{7.5}$$

Let us now consider the case where the electrical vector is oriented along the **x**-axis. The polarizability in the **x** direction (p_{xx}) becomes:

$$p_{xx} = p_1\cos^2\alpha + p_2\sin^2\alpha \tag{7.6}$$

which, since $\cos\alpha = \cos\upsilon\sin\phi$, may be modified to:

$$p_{xx} = p_2 + \left(p_1 - p_2\right)\sin^2\phi\cos^2\upsilon \tag{7.7}$$

The polarizability tensor ($\mathbf{p}_{ij}$) can be converted to the corresponding refractive index tensor ($\mathbf{n}_{ij}$) according to the Lorentz-Lorenz equation:

$$\frac{n_{ij}^2 - 1}{n_{ij}^2 + 2} = \left(\frac{4\pi}{3}\right) p_{ij} \tag{7.8}$$

Insertion of Eqs. (7.6) and (7.7) in Eq. (7.8) yields the expressions:

$$\frac{n_{zz}^2 - 1}{n_{zz}^2 + 2} = \left(\frac{4\pi}{3}\right)\left(p_1 \cos^2\phi + p_2 \sin^2\phi\right) \tag{7.9}$$

$$\frac{n_{xx}^2 - 1}{n_{xx}^2 + 2} = \left(\frac{4\pi}{3}\right)\left(p_2 + (p_1 - p_2)\sin^2\phi\cos^2\upsilon\right) \tag{7.10}$$

The birefringence (Δn) and the average refractive index $\langle n \rangle$ are defined as follows:

$$\Delta n = n_{zz} - n_{xx} \tag{7.11}$$

$$\langle n \rangle = \frac{1}{2}\left(n_{xx} + n_{zz}\right) \tag{7.12}$$

Combination of Eqs. (7.11) and (7.12) yields the expressions:

$$n_{xx} = \langle n \rangle - \frac{\Delta n}{2} \tag{7.13}$$

$$n_{zz} = \langle n \rangle + \frac{\Delta n}{2} \tag{7.14}$$

Subtraction of Eq. (7.10) from Eq. (7.10) yields:

$$\frac{n_{zz}^2 - 1}{n_{zz}^2 + 2} - \frac{n_{xx}^2 - 1}{n_{xx}^2 + 2} = \frac{6\langle n \rangle \Delta n}{\left(n_{zz}^2 + 2\right)\left(n_{xx}^2 + 2\right)} \approx \frac{6\langle n \rangle \Delta n}{\left(\langle n \rangle^2 + 2\right)^2} \tag{7.15}$$

Insertion of Eqs. (7.9) and (7.10) into Eq. (7.15) yields, after algebraic simplification, the following expression:

$$\Delta n = \frac{\left(\langle n \rangle^2 + 2\right)^2}{6\langle n \rangle} \cdot \frac{4\pi}{3} \cdot \left(p_1 - p_2\right) \cdot \left(1 - \sin^2\phi - \cos^2\upsilon \sin^2\phi\right) \tag{7.16}$$

A great number of segments are considered and the assumption made at this stage is that orientation is *uniaxial*. All angles υ are equally probable. The average square of the cosine of υ may be calculated as follows:

$$\left\langle \cos^2 \upsilon \right\rangle = \frac{1}{2\pi} \int_0^{2\pi} \cos^2 \upsilon = \frac{1}{2} \tag{7.17}$$

Insertion of Eq. (7.17) in Eq. (7.16) and averaging for all segments over all theta angles give:

$$\Delta n = \frac{\left(\langle n \rangle^2 - 2 \right)^2}{6 \langle n \rangle} \cdot \frac{4\pi}{3} \cdot (p_1 - p_2) \cdot \left(1 - \frac{3 \langle \sin^2 \phi \rangle}{2} \right) \tag{7.18}$$

Hermans orientation function (*f*) is defined as

$$f = \frac{\Delta n}{\Delta n_0} = 1 - \frac{3}{2} \langle \sin^2 \phi \rangle = \frac{3 \langle \cos^2 \phi \rangle - 1}{2} \tag{7.19}$$

where the maximum (intrinsic) birefringence Δn_0 is given by

$$\Delta n_0 = \frac{\left(\langle n \rangle^2 - 2 \right)^2}{6 \langle n \rangle} \cdot \frac{4\pi}{3} \cdot (p_1 - p_2) \tag{7.20}$$

The Hermans orientation function (*f*) takes the value 1 for a system with complete orientation parallel to the director and it takes the value -1/2 for the very same sample with the director perpendicular to the chain axis (Fig. 7.5). Non-oriented samples have an *f* value equal to zero.

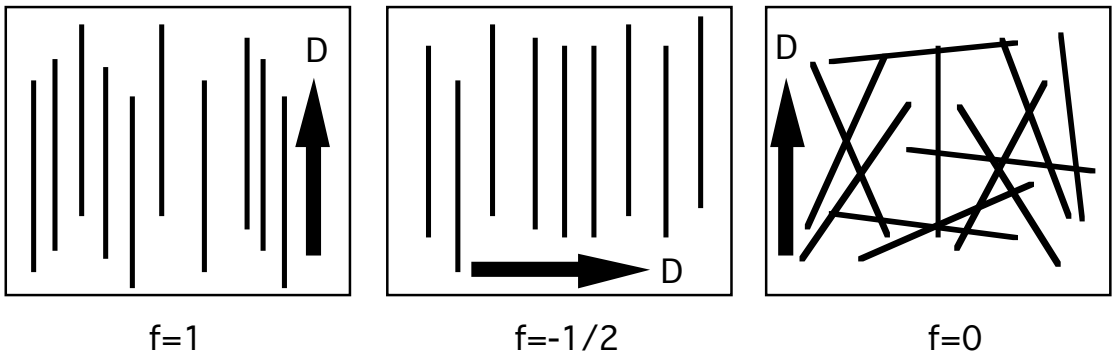

Fig. 7.5. Values for the Hermans orientation function for three simple cases. The director (D) is shown for each case.

It is possible to obtain estimates of the orientation function (*f*) by a number of methods other than birefringence measurements, e.g. X-ray diffraction or infrared spectroscopy.

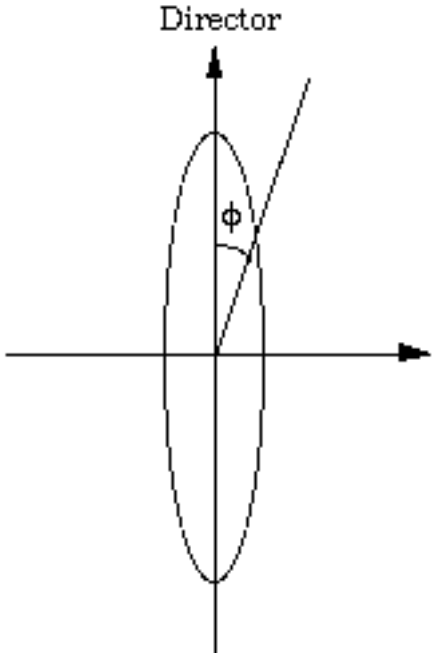

Fig. 7.6. Illustration of orientation function f(ϕ). The orientation is a density function of only one parameter

The orientation can be viewed in more general terms (Fig. 7.6). Let us represent the orientation by an orientation probability function $f(\phi)$, where the angle ϕ is the angle between the director and the molecular segment. It is implicit in this statement that the orientation in the plane perpendicular to the director is random, i.e. orientation is uniaxial. It is possibly to represent $f(\phi)$ by a series of spherical harmonics (Fourier series), and it can be shown that the following equation holds:

$$f(\phi) = \sum_{n=0}^{\infty} \left(n + \frac{1}{2} \right) \langle f_n \rangle f_n(\phi) \tag{7.21}$$

where the odd components are all zero and the first three even components are given by:

$$f_2(\phi) = \frac{1}{2}\left(3\cos^2\phi - 1\right) \tag{7.22}$$

$$f_4(\phi) = \frac{1}{8}\left(35\cos^4\phi - 30\cos^2\phi + 3\right) \tag{7.23}$$

$$f_6(\phi) = \frac{1}{6}\left(231\cos^6\phi - 15\cos^4\phi + 105\cos^2\phi - 5\right) \qquad (7.24)$$

The parameters $\langle f_n \rangle$ are the average values (amplitudes). Note that f_2 is the Hermans orientation function. The full description of uniaxial orientation $f(\phi)$ cannot thus be attained by a single measurement of birefringence. Hermans orientation function can be given a simple interpretation. A sample with orientation f may be considered to consist of perfectly aligned molecules of the mass fraction f and randomly oriented molecules of the mass fraction 1-*f*. Liquid crystalline polymers are often characterized by their order parameter (denoted *S*). This quantity is equivalent to the Hermans orientation function.

Polymers may exhibit a biaxial orientation. The segmental orientation function is in this case a function of two angular variables, i.e. $f(\phi,\upsilon)$. The measurement of the biaxial case is discussed in section 7.4.

7.3. Methods for the assessment of uniaxial chain orientation

There are several methods, which are commonly used for the determination of chain orientation: e.g. measurement of in-plane birefringence, wide-angle X-ray diffraction, small-angle X-ray diffraction, infrared spectroscopy and sonic modulus measurements. The first four are briefly presented in this section. Recommended reading for a more in-depth understanding is given at the end of the chapter.

We deal in this section only with the simplest case, namely uniaxial orientation (Fig. 7.7). There is only one unique direction, the **z** (3) direction. Orientation 'exists' only in the **xz**- and **yz**-planes. The uniaxial system appears to be isotropic in the **xy**-plane.

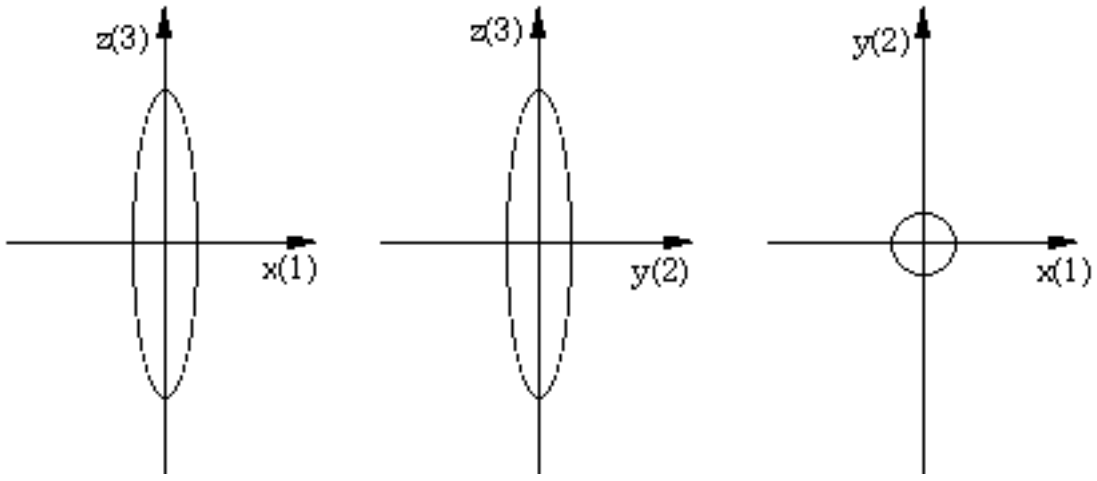

Fig. 7.7.Uniaxial orientation

7.3.1. Birefringence

Birefringence measurements are classical. The Hermans orientation function (f) is proportional to the birefringence (Δn) according to:

$$f = \frac{\Delta n}{\Delta n_0} \tag{7.25}$$

where Δn_0 is the maximum birefringence. The latter (Δn_0) can take negative or positive values. Polymers with polarizable units in the main chain, e.g. polyethylene and poly(ethylene terephthalate) have positive Δn_0-values, whereas polymers with strongly polarizable pendant groups, e.g. polystyrene show negative Δn_0-values. The measured Δn can be the result of contributions from several components (phases), from internal stresses (deformations) and from interfacial effects (so-called form birefringence)

$$\Delta n = \Delta n_{\mathrm{f}} + \Delta n_{\mathrm{d}} + \Delta n_{\mathrm{c}} + \Delta n_{\mathrm{a}} \tag{7.26}$$

where Δn_{f} is the form birefringence, Δn_{d} is the deformation birefringence, and Δn_{c} and Δn_{a} are the orientation-induced birefringences originating from the crystalline and the amorphous components. Form birefringence occurs only in multiphase systems. The general conditions for it to occur are that the phases have different refractive indices, that at least one of the dimensions of the dispersion is of the order of the wavelength of the light, and that the shape of the multiphase structure is anisotropic. Folkes and Keller (1971) showed that an unoriented block-copolymer of polystyrene and polybutadiene exhibited a pronounced form birefringence. The polystyrene-rich phase consisted of thin (30 nm) cylinders dispersed in the matrix of the polybutadiene-rich phase. Semicrystalline polymers may also exhibit form birefringence. Bettelheim and Stein (1958) have indicated that the form effects may constitute 5-10% of the total birefringence in polyethylene. Other researchers, e.g. Samuels (1974), claimed that the form birefringence in oriented isotactic polypropylene is insignificant. Deformation may cause stresses in bonds, which also lead to birefringence. This deformation birefringence is usually insignificant and is mentioned only for completeness.

If orientation is uniaxial and both form and deformation birefringence can be neglected, the previous equation can be rewritten:

$$\Delta n = \Delta n_{\mathrm{c}} + \Delta n_{\mathrm{a}} = \Delta n_0 \left[w_{\mathrm{c}} f_{\mathrm{c}} + \left(1 - w_{\mathrm{c}}\right) f_{\mathrm{a}} \right] \tag{7.27}$$

where f_c and f_a are the Hermans orientation functions of the crystalline and the amorphous components and w_c is the crystallinity.

Birefringence measurements can be made in a polarized light microscope using the configuration described in Fig. 7.9. Analyser and polarizer should be crossed and should be oriented at an angle of 45° to the main optical axes of the sample. A compensator, a component made of birefringent material, is introduced between the sample and the analyser. The compensator makes it possible to change the optical retardation of the vertically and horizontally polarized light components so that the optical retardation introduced by the sample is compensated for. There are different types of compensators. The Babinet and the tilt compensators are probably the most common.

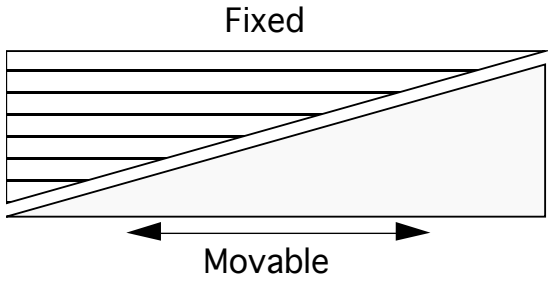

Fig. 7.8. Babinet compensator which consists of two quartz wedges with crossed optical axes

The Babinet compensator consists of two quartz wedges cut so that their optical axes are mutually perpendicular (Fig. 7.8). A longitudinal shift of the lower wedge changes the optical retardation (R_{31}). A series of fringes is observed around the centre provided that monochromatic light has been used. The longitudinal shift of the lower wedge which shifts the zero-order fringe to the centre gives, after suitable calibration, R_{31} of the sample. With a white light source, containing a continuous spectrum of energy in wavelengths from 400 nm to 750 nm, coloured fringes are observed on both sides of the central black fringe with an optically isotropic sample. The optical retardation is wavelength-dependent and the complex subtraction of light of different wavelengths means that each optical retardation is characterized by a specific colour. This colour scale, i.e. colour as a function of optical retardation, is given in the Michel-Levy chart.

The tilt compensators consist of either a single birefringent calcite plate (Berek type) or two plates of either calcite or quartz cemented together (Ehringhaus compensator). The change in optical retardation is achieved by rotation of the plate, which causes a change in both absolute travelling length and refractive index.

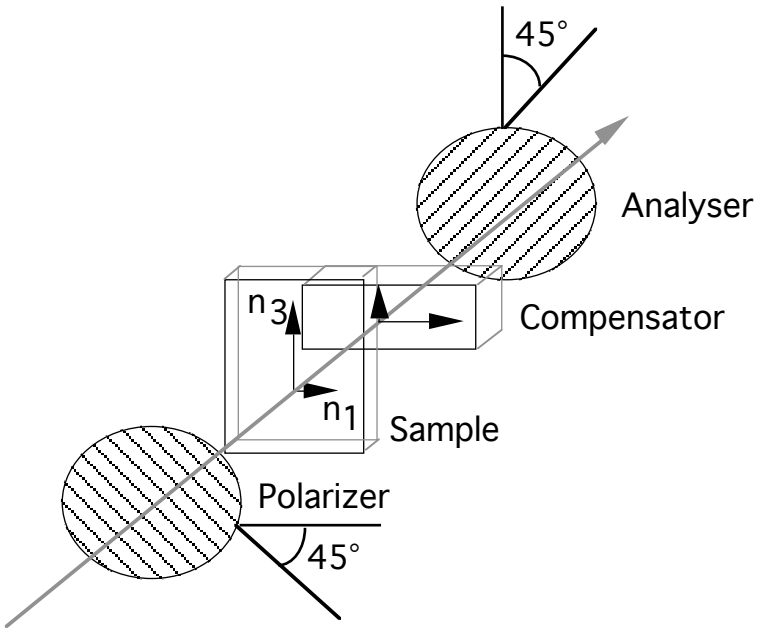

Fig. 7.9. Optical system for the measurement of orientation in the plane.

The in-plane birefringence ($\Delta n=n_3-n_1$) is calculated from the measured optical retardation (R_{31}) according to:

$$\Delta n = \frac{R_{31}\lambda}{d} \tag{7.28}$$

where λ is the wavelength of the light and d is the sample thickness. The compensator method is ideal for static measurements. For dynamic measurements, it is possible to remove the compensator and to measure the intensity of the transmitted light (I) from which the optical retardation (R_{31}) can be calculated:

$$I = I_0 \sin^2\left(\pi R_{31}\right) \tag{7.29}$$

where I_0 is the intensity of the incoming light. This equation is only applicable to samples showing an optical retardation less than the wavelength of the light. The in-plane birefringence can then be calculated according to Eq. (7.28).

Optically clear amorphous polymers are readily studied also using relatively thick samples. However, semi-crystalline polymers scatter light and the method of using visible light is only applicable to the study of thinner samples (<100 μm). Thicker samples (mm thickness) of polyethylene have been studied with far-infrared interferometry.

7.3.2. Wide-angle X-ray diffraction

The in-plane orientation of (hkl) planes in semi-crystalline polymers is revealed by wide-angle X-ray diffraction. Fig. 7.10 shows the diffraction patterns of two samples of the same polymer. The unoriented polymer shows concentric rings for the intra-chain (00l) and inter-chain (hk0) reflections. The oriented polymer shows diffractions of both (00l) and (hk0), which are strongly dependent on the azimuthal angle (ϕ). The intra-chain reflection is concentrated to the meridian and the inter-chain reflection to the equator.

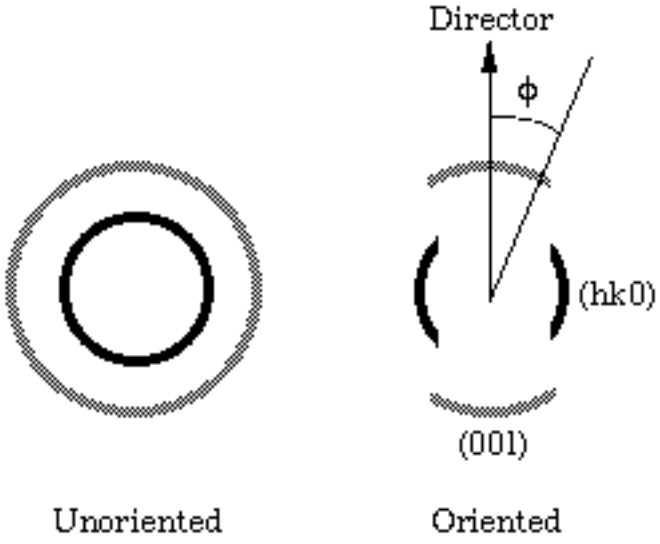

Fig. 7.10. Schematic X-ray diffraction patterns from an unoriented and an oriented crystalline polymer. Definition of the azimuthal angle ϕ.

The orientation expressed by the average square of the cosine of angle ϕ of the diffracting planes (hl0) and (00l) can be calculated from the equation:

$$\left\langle \cos^2 \phi_{hkl} \right\rangle = \frac{\int_0^{\pi} I_{hkl}(\phi) \cdot \cos^2 \phi \cdot \sin \phi \cdot d\phi}{\int_0^{\pi} I_{hkl}(\phi) \cdot \sin \phi \cdot d\phi} \qquad (7.30)$$

where $I_{hkl}(\phi)$ is the scattered intensity of the (hkl) reflection at the azimuthal angle ϕ. It is here assumed that orientation is uniaxial. The sin ϕ factor originates from the fact that the number of populating diffracting crystals increases with the radius of the circle, i.e. with sin ϕ (Fig. 7.11).

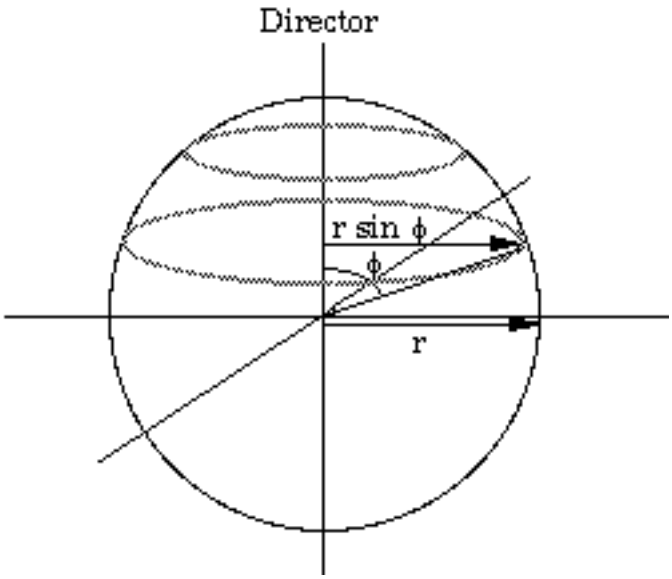

Fig. 7.11. Illustration of the dependence of the number of diffracting planes on the angle ϕ

The following expression relating the orientation of the different crystal planes (100), (010) and (001) of an orthorhombic cell to a common director holds:

$$\left\langle \cos^2 \phi_{100} \right\rangle + \left\langle \cos^2 \phi_{010} \right\rangle + \left\langle \cos^2 \phi_{001} \right\rangle = 1 \tag{7.31}$$

Eq. (7.31) may be applied to the simple case shown in Fig. 7.10 with only one inter-chain reflection:

$$2\left\langle \cos^2 \phi_{hk0} \right\rangle + \left\langle \cos^2 \phi_{001} \right\rangle = 1 \tag{7.32}$$

Eqs. (7.31) and (7.32) are readily transformed into the corresponding Hermans orientation functions (f_{hkl}):

$$f_{100} + f_{010} + f_{001} = 0 \tag{7.33}$$

and

$$2f_{hk0} + f_{001} = 0 \tag{7.34}$$

One of the main attractions of the X-ray method is that the orientation function of crystalline planes, $f(\phi)$ in the case of uniaxial orientation and $f(\phi,\upsilon)$ in the case of biaxial orientation, can be revealed. The orientation can also be expressed in the Hermans orientation function. X-ray diffraction primarily assesses crystalline orientation. However, the amorphous halo may show azimuthal-angle-dependence and, the amorphous orientation can be estimated provided that a certain amorphous peak can be assigned to either an inter-chain or an intra-chain spacing,

7.3.3. Small-angle X-ray diffraction

Small-angle X-ray diffraction provides information about the period of the lamella stacking in semi-crystalline polymers and about the layer thickness of smectic liquid crystalline polymers. The azimuthal-angle dependence of the small-angle pattern provides information about the orientation of these 'super-structures' (Fig. 7.12).

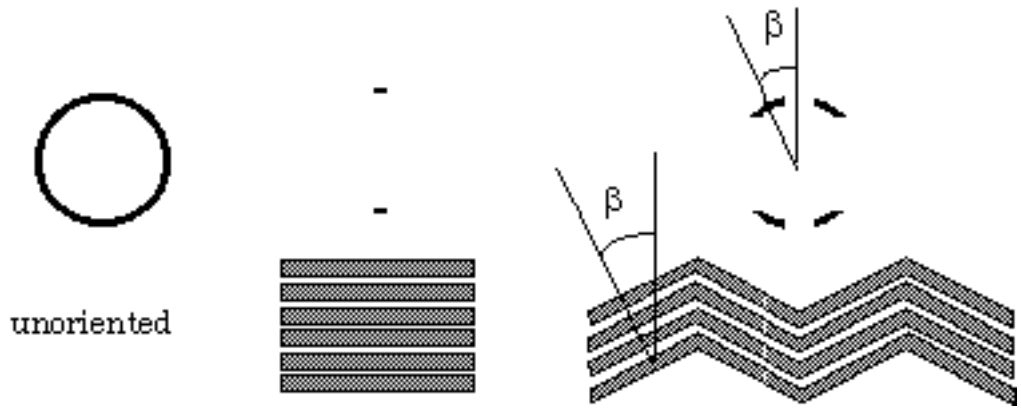

Fig. 7.12. Small-angle X-ray patterns of different lamella organizations

The two-point pattern indicates that the lamella planes are perpendicular to the director. The orientation of these lamellar structures can be calculated from Eq. (7.30). The four-point pattern indicates that the lamella normal scatters around an angle β to the director.

7.3.4. Infrared (IR) spectroscopy

IR spectroscopy is very useful for the assessment of chain orientation. The measurement of IR dichroism requires the use of IR radiation with parallel and perpendicular polarization to a selected reference direction. Fig. 7.13 shows the fundamental principle underlying the dichroism.

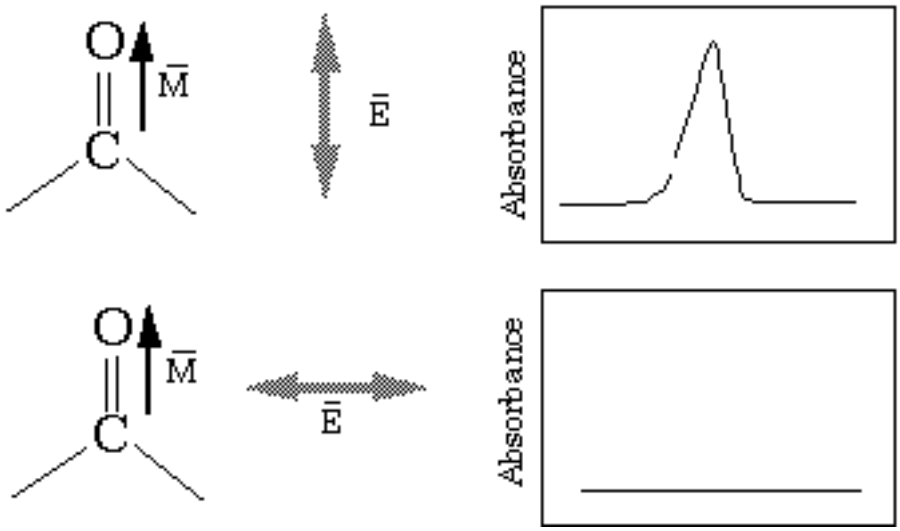

Fig. 7.13. Absorption of infrared light of different polarization ($\overline{E}$) with respect to the transition moment vector ($\overline{M}$)

The theory developed by Beer predicts that the absorbance (*A*) depends very strongly on the angle (κ) between the electric vector and the transition moment vector:

$$A \cong \left[\left|\overline{E}\right| \cdot \left|\overline{M}\right| \cdot \cos\kappa \right]^2 \tag{7.35}$$

The IR radiation is strongly absorbed when the electric vector and the transition moment vector are parallel (Fig. 7.13). In the case of perpendicular orientation, no absorption occurs (Fig. 7.13). The dichroic ratio (*R*) is defined as:

$$R = \frac{A_{\text{II}}}{A_{\perp}} \tag{7.36}$$

where A_{II} is the absorbance of polarized light parallel to the director and $A_{\perp}$ is the absorbance of polarized light perpendicular to the director. Hermans orientation function (*f*) is given by:

$$f = \frac{(R-1)\cdot(R_0+2)}{(R+2)\cdot(R_0-1)} \tag{7.37}$$

where R_o is the dichroic ratio for a sample with perfect uniaxial orientation and is dependent on the angle between the transition moment vector and the chain axis (ψ, Fig. 7.14):

$$R_0 = \cot^2 \psi \tag{7.38}$$

Absorption bands with ψ=54.76° show no dichroism (R_0=1). Absorption bands associated with a perpendicular transition moment vector have R_0=0 and the Hermans orientation function is given by:

$$f = 2 \cdot \frac{(1-R)}{(R+2)} \tag{7.39}$$

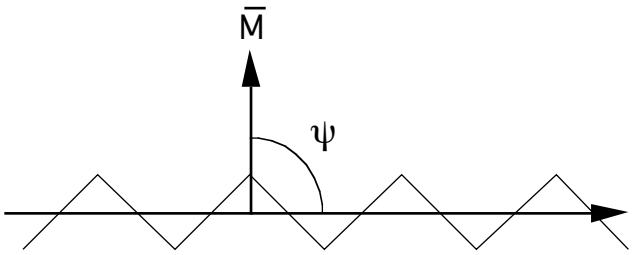

Fig. 7.14. Definition of angle between transition moment vector and chain axis

One of the attractions of the IR technique is that the dichroism of the absorption bands assigned to different groups can be determined and that the orientation of different groups of the repeating unit can be determined. The orientation of a side-chain smectic poly(vinyl ether) (Fig. 7.15) was measured by Gedde et al. (1993). The cyano-stretching band at 2230 cm^{-1} with a transition moment vector parallel to the long axis of the mesogen showed a dichroic ratio corresponding to f=0.7-0.8, whereas the symmetric and asymmetric CH-stretching bands at 2854 cm^{-1} and 2927 cm^{-1} associated essentially with the spacer showed that the spacer group was considerable less oriented, f=0.3-0.4.

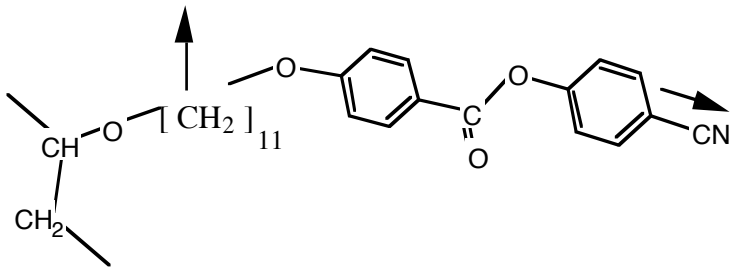

Fig. 7.15. Structure of repeating unit of side-chain polyvinylether. Approximate directions of the transition moment vectors are indicated.

The dichroic ratio can also be measured using ultraviolet or visible radiation (UV-visible spectroscopy). Polymers with carbonyl groups, phenyl groups and other conjugated systems may be studied.

7.3.5. Sonic modulus

The velocity of sound depends on the modulus, and the velocity of sound is greater when it propagates along than transverse to the chain axis. In a semi-crystalline polymer, both the crystals and the amorphous phase contribute in proportion to their relative contents. In that sense, the sonic modulus is similar to birefringence. The following expression relating sonic modulus (E) and Hermans orientation factor for a semicrystalline polymer was derived by Samuels (1974):

$$\frac{3}{2}\left(\frac{1}{E}-\frac{1}{E_{\mathrm{u}}}\right)=\frac{v_{\mathrm{c}}f_{\mathrm{c}}}{E_{\mathrm{t,c}}}+\frac{\left(1-v_{\mathrm{c}}\right)f_{\mathrm{a}}}{E_{\mathrm{t,a}}} \tag{7.40}$$

where E_{u} is the modulus of the unoriented polymer, v_{c} is the volume crystallinity, f_{c} and f_{a} are the Hermans orientation functions of the crystalline and amorphous components, and $E_{\mathrm{t,c}}$ and $E_{\mathrm{t,a}}$ are the moduli for the propagation of the sound perpendicular to the chain in the crystalline and the amorphous fractions.

7.3.6. Amorphous and crystalline orientation

Eq. (7.27) states that the overall orientation of a semi-crystalline polymer is the sum of contributions from the amorphous and crystalline components. The overall orientation (f) can be obtained by measurement of birefringence or the sonic modulus, and the crystalline orientation (f_c) can be obtained by wide-angle X-ray diffraction. The amorphous orientation (f_a) can then be obtained indirectly according to:

$$f_{\mathrm{a}}=\frac{f-f_{\mathrm{c}}w_{\mathrm{c}}}{1-w_{\mathrm{c}}} \tag{7.41}$$

It is relatively difficult to make a direct determination of the amorphous orientation function of a semi-crystalline polymer. Determination by X-ray diffraction recording the azimuthal-angle-dependence of the amorphous halo and infrared dichroism of an amorphous absorption band may be useful in addition to the indirect method suggested above.

7.4. Methods for the assessment of biaxial chain orientation

Biaxiality is illustrated in Fig. 7.16. In this case, it is possible to find two orthogonal planes in both of which the chains have a preferential direction. The orientation function is a function of two angular variables.

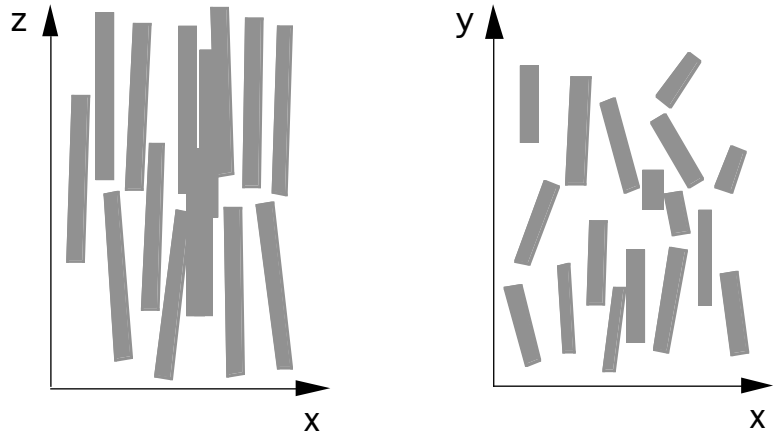

Fig. 7.16. Schematic drawing showing the orientation of uniaxial moieties in two orthogonal planes.

The biaxial orientation can be assessed by optical methods measuring the in-plane birefringence in the three orthogonal directions. The three Δn-values may be derived by tensor summation of Eq. (7.16):

$$n_3 - n_1 = \Delta n_0 \left(f - \frac{g}{2} \right) \tag{7.42}$$

$$n_3 - n_2 = \Delta n_0 \left(f + \frac{g}{2} \right) \tag{7.43}$$

$$n_1 - n_2 = \Delta n_0 g \tag{7.44}$$

where $f = \frac{1}{2}\left(3\left\langle \cos^2 \phi \right\rangle - 1\right)$ and $g = \left\langle \sin^2 \phi \cdot \cos 2\upsilon \right\rangle$

X-ray diffraction can also be used, the X-ray diffraction patterns being recorded at different angles. It is in principle possible to obtain the complete crystalline orientation function (= $f(\phi,\upsilon)$). Biaxiality may not only refer to the chain axis. In a single crystal of polyethylene, for example, the chain orientation is indeed very high (f typically greater

than 0.95), but the single-crystal also shows equally significant a-axis and b-axis orientations. These "secondary" bond orientations are obviously less important for properties because the largest difference found is that between the covalent bond and the secondary bond. However, certain variations in properties arise from a-axis and b-axis orientation, particularly in cases involving very strong secondary bonds. e.g. hydrogen bonds.

7.5. How chain orientation is created

The methods by which chain orientation is created may be divided into solid-state and liquid processes. The solid-state processes involve a plastic deformation of an isotropic or weakly anisotropic solid. Glassy amorphous polymers can only be drawn to moderate strains. The polymers, which can be substantially oriented are semi-crystalline with deformable amorphous ($T>T_g$) and crystalline phases. The remaining discussion in this section is confined to this group of polymers. Deformation can be achieved by cold-drawing, extrusion or rolling (Fig. 7.17).

Cold-drawing leads to necking, the formation of a localized zone in which the 'unoriented' structure is transformed into a fibrous structure. The neck zone, i.e. the shoulder, travels through the specimen until the entire sample is drawn to a fibrous structure. A commonly used parameter that characterizes the extent of drawing is the draw ratio (λ):

$$\lambda = \frac{L}{L_0} \approx \frac{A_0}{A} \tag{7.45}$$

where L is the specimen length after drawing, L_0 is the original specimen length, A_0 is the original cross-sectional are and A is the cross-sectional area after drawing. The necking also causes the formation of a great many voids. Due to these voids the cold-drawn fibrous material is thus often opaque. The draw ratio reached after necking is denoted the natural draw ratio and it takes values between 4 and 10. Polymers of suitable morphology can be drawn after necking to very high draw ratios, e.g. to λ=40 for linear polyethylene. In many cases, these very high draw ratios can only be attained by drawing at elevated temperatures, typically 10-40°C below the melting point.

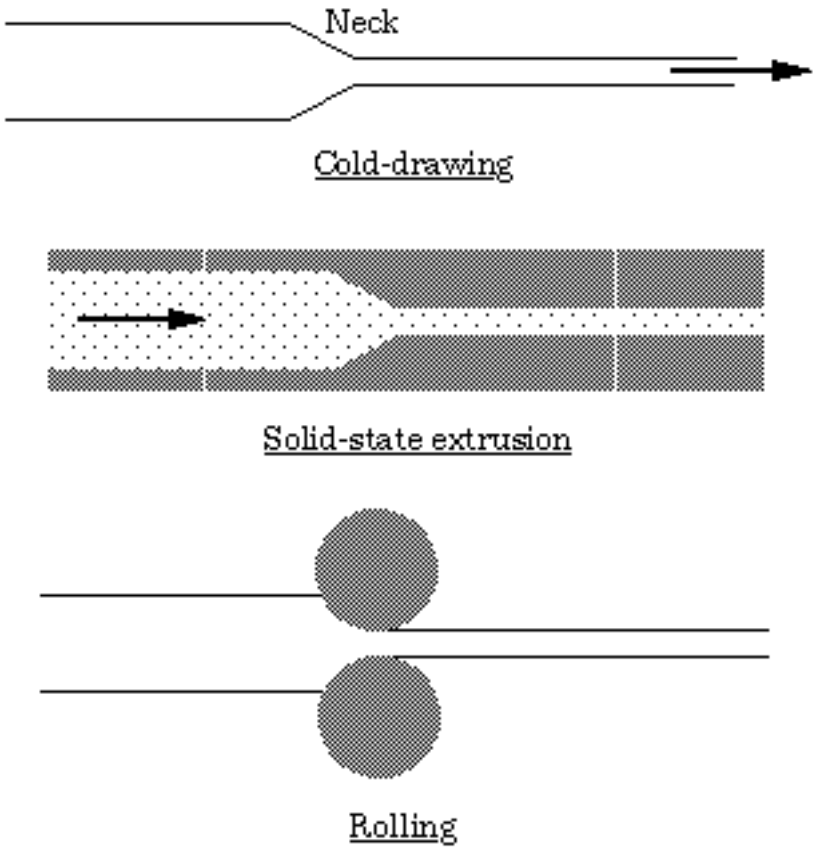

Fig. 7.17. Solid-state processes to orient a polymer

During solid-state extrusion, the solid polymer is pushed through a narrow hole and a very significant pressure is built up. A plug of solid polymer is pushed through the hole in the cold extrusion process, whereas the solid plug is surrounded by a pressure-transmitting oil in the case of hydrostatic extrusion. Solid-state extrusion to high draw ratios is only possible at temperatures above the onset temperature for the crystalline α process. Linear polyethylene is extruded at temperatures between 80°C and 110°C. The entrance angle is important. Small angles leads to slow deformation and a possibility for the material to return to the unoriented state by relaxation. Higher entrance angles cause more rapid deformation and a higher efficiency of the orientation process. Fracture may occur when very high entrance angles are used. Zachariades, Mead and Porter (1979) developed an extrusion process, which was intermediate between the solid-like and liquid-like processes. The hydrostatic extrusion of polyethylene was performed at 132°C to 136°C and above a certain critical deformation rate. The pressure increased rapidly, which promoted oriented crystallization in the capillary entrance. The output of this process was a highly oriented and optically clear fibre.

The ability of a polymer to be drawn or extruded to an ultra-oriented fibre is dependent on several material factors:

- The presence of a crystalline α relaxation is a necessary condition for the possibility to extrude a polymer to a high draw ratio. The α process involves slippage of the chains through the crystals, and polymers having this ability also tend to be able to deform plastically into a highly oriented morphology. Polyamides exhibit no crystalline α process and solid-state extrusion of polyamide 6 is only possible at small draw ratios. Drawing or extrusion is preferably carried out at a temperature between the temperature of onset of the α process and the melting temperature.

- Chain entanglements make the plastic deformation difficult and high molar mass polymers crystallized under normal conditions cannot be drawn to very high draw ratios. It is also known that crystallization conditions leading to the formation of only very few chain entanglements favour extensibility and the attainment of an ultra-oriented fibre.

- The number of interlamellar tie chains must be sufficiently high to prevent early brittle fracture.

Cold-drawing/solid state extrusion of semicrystalline polymers involves initially the deformation of the spherulitic structure, the subsequent transformation of the spherulitic structure to a fibrillar structure and finally the plastic deformation of the fibrillar structure. The most intriguing part is the transformation stage. It was suggested by Peterlin (1979), one of the pioneers of the field, that the crystal lamellae twist (rotate) and break up into smaller crystallites, which are pulled into long and thin microfibrils (a sandwich consisting of 10 nm thick and wide crystal blocks connected with many taut tie chains). This mechanism seems not to account for the observed change in the crystal thickness accompanying the transformation process. Peterlin showed in the 1970's that the crystal thickness (L_c) of the fibrous polymer depends on the degree of supercooling (ΔT) prevailing during the transformation of the spherulitic to a fibrillar structure, according to an expression valid for any crystallization, viz.:

$$L_c = \frac{C_1}{\Delta T} + C_2 \qquad (7.46)$$

where C_1 and C_2 are constants. The validity of Eq. (7.46) indicated that both melting and recrystallization accompanied the transformation. Sadler and Barham (1990) showed in a recent study by small-angle neutron scattering that cold-drawing of linear polyethylene at temperatures greater than 70-90°C indeed involved melting and recrystallization. However, at temperatures lower than 70-90°C, no melting occurred

and the ΔT-dependence of the crystal thickness must be explained differently. Sadler and Barham suggested that laterally small crystalline blocks are broken out from the crystal lamellae so that the regular stacking is partially lost. The small-angle X-ray diffraction pattern is smeared out. Furthermore, Sadler and Barham suggested that the thinner crystals are not disintegrated to the same extent but instead rotate to adapt to the fibrillar orientation, leaving the regularity of the lamella stacking and providing the small-angle X-ray diffraction patterns recorded. Sadler and Barham also found that the transformation of the melt-crystallized spherulitic structure to a fibrillar structure was accomplished by affine deformation of the molecules. The molecular draw ratio was thus the same as the measured macroscopic draw ratio. Drawing of single crystal mats of polyethylene led however to non-affine deformation during necking.

The phenomenon of necking is closely related to that of yielding. Fig. 7.18 shows that the yield stress is strictly proportional to the crystal thickness and that the regression line intersects the axes at the origin. The yield stress increases with increasing mass crystallinity (at constant crystal thickness). It may be concluded that the yield as a precursor to necking is controlled by deformation within the crystals. The exact mechanism for the yielding of semicrystalline polymers is not known but several proposals have been made: intralamellar slip along chain axis involving different (hk0) planes, twinning, and thermal activations of screw dislocations.

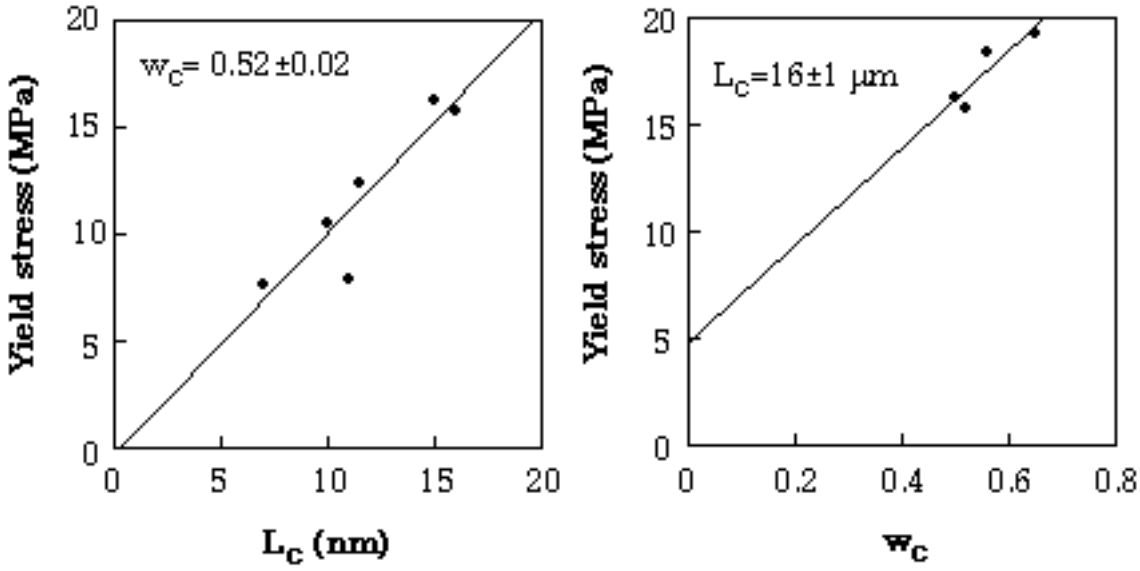

Fig. 7.18. Yield stress of polyethylene as a function of crystal thickness (L_c) at constant crystallinity (w_c=0.52) and as a function of mass crystallinity (w_c) at constant crystal thickness (L_c= 16 nm). Drawn after data from Young (1988).

Sadler and Barham (1990) also recorded the change in molecular draw ratio during the post-necking deformation and found that it was equal to the change in the measured macroscopic draw ratio. Post-necking deformation is thus affine. Earlier data by

electron microscopy and Raman spectroscopy of ultra-oriented cold-drawn or solid-state extruded polyethylene indicated the presence of extended-chain fibrillar crystals together with oriented folded chain crystals. It is believed that this longitudinal continuity of the molecules has a profound positive effect on the stiffness of the fibre.

The liquid processes include melt-spinning and solution-spinning. The melt or the solution is strained and the molecules are extended from their equilibrium isotropic shapes. High molar mass species show the longest relaxation times and are the most likely to crystallize while being oriented and hence to form extended-chain crystals. Later crystallizing species form epitaxial folded-chain lamellae. The success of a 'liquid process' is strongly dependent on the oriented state being frozen-in with a minimum of relaxation. The mobile oriented liquid may be quenched by a rapid elevation of the hydrostatic pressure or by rapid cooling. The resulting morphology is denoted 'interlocked shish-kebab'. The melt-drawing process was developed for high molar mass polyethylene by Mackley and Keller (1973) and an axial modulus approaching 100 GPa was achieved in the best cases. Kevlar (polyterephthalamide) is spun from a solution in concentrated sulphuric acid. The solution shows nematic mesomorphism and is readily oriented.

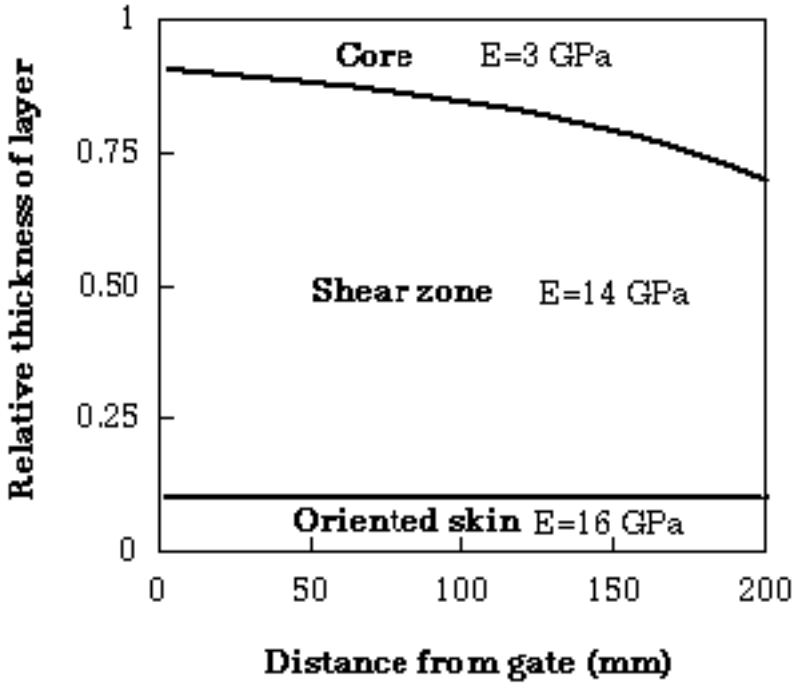

Fig. 7.19. Relative thickness of microstructural layers of a 3 mm thick injection-moulded ruler of liquid-crystalline poly(p-hydroxybenzoic acid-co-ethylene terephthalate). The axial modulus (E) of the materials in the different layers are shown. Drawn after data from Hedmark et al. (1988).

Injection moulding causes a more moderate orientation of the material near the surfaces of the mould. The chain orientation is generally along the major flow direction. Fig. 7.19 shows the structural layering of a liquid crystalline polymer. The outermost layer is formed by elongational flow. The orientation within the next layer is due to shear flow. Conventional polymers show principally a similar orientation pattern although the orientation is weaker and the thickness of the oriented layers is considerably smaller than that of liquid crystalline polymers.

Finally, a few words about other methods used to achieve orientation: Electrical and magnetic fields have been used to align both monomers, particularly liquid crystalline, and polymers. The field strength needed to orient polymers is very high, several orders of magnitude greater than that required to orient small molecules.

7.6. Properties of oriented polymers

The first question asked in this section is 'what are the properties of a perfectly aligned polymer'. Large samples showing perfect orientation have not been prepared. The properties are either measured on a very small piece, e.g. a single crystal (crystallite), or are calculated from other measurements. The highest possible axial elastic modulus of a polymer can be experimentally determined from X-ray diffraction data by measuring the change in the distance between crystal planes in accurately stressed crystallites. It can also be calculated from data obtained by vibrational spectroscopy. The latter provides data on the elastic constants of the individual bonds deformed by stretching, and the bond angle deformation, and a theoretical modulus can be calculated. The axial and transverse thermal expansivities are readily obtained from X-ray diffraction data. Table 7.1 presents axial (along chain axis) elastic modulus data for a few selected polymers.

Table 7.1. The maximum elastic modulus at room temperature of a few selected polymers[a]

Polymer	Elastic modulus (GPa)
Polyethylene	240-360
Isotactic polypropylene	42
Polyoxymethylene	54
Poly(ethylene terephthalate)	140
Polyamide-6	250
Diamond	800

Source: Holliday and White (1971).

A simple but very useful principle is to consider that the elastic deformation of a single molecule occurs by three possible mechanisms (Fig. 7.20): bond stretching, bond-angle deformation and torsion about a σ bond. The elastic constants for these three deformation mechanisms are very different. The following comparative values may be used: 100 (bond stretching), 10 (bond angle deformation) and 1 (torsion about a σ bond).

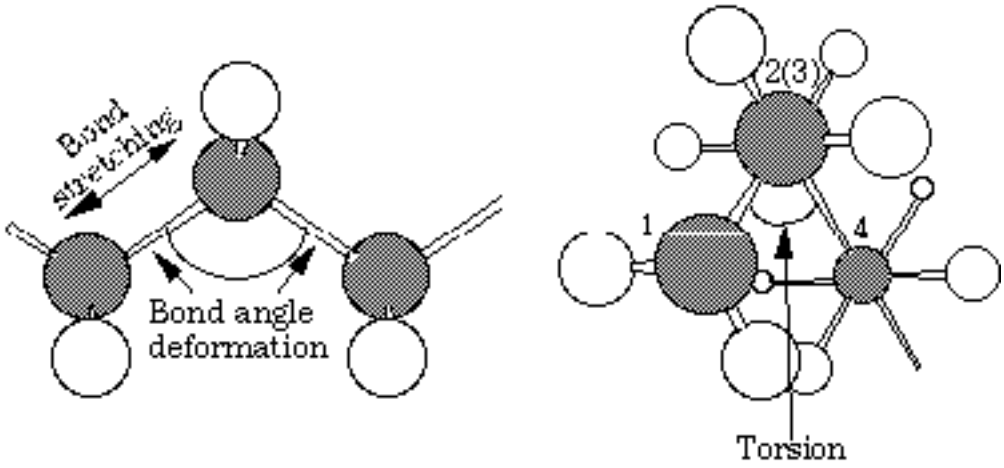

Fig. 7.20. Deformation of a polyethylene molecule by bond stretching, bond angle deformation (both left-hand side) and torsion about the σ bond linking carbons 2 and 3 (right-hand side).

The high axial elastic modulus of polyethylene and polyamide 6 is due to the fact that these polymers have a preferred conformation that is fully extended, i.e. all-trans. The elastic deformation is caused by the deformation of bond angles and by bond stretching, both showing high elastic constants. Isotactic polypropylene and polyoxymethylene crystallize in helical conformations and therefore exhibit a maximum stiffness which is only 20% of the maximum stiffness of the all-trans polymers. The elastic deformation of a helical chain involves, in addition to the deformation of bond angles and bond stretching, also deformation by torsion about the s bonds. The latter shows a very low elastic constant. The relatively low maximum stiffness of the fully extended (all-trans) poly(ethylene terephthalate) is due the low molecular packing of this polymer. The three-dimensional covalent-bond-structure of diamond leads to its extraordinarily high stiffness by largely inhibiting bond angle deformation.

The transverse modulus is determined by the weak secondary bonds and is for this reason only a small fraction of the axial (along chain) elastic modulus. X-ray diffraction indicates the following values for linear polyethylene: $E_c \approx$ 300 GPa and $E_a \approx E_b \approx$ 3 GPa. Polar polymers with stronger *inter*molecular bonds show higher transverse moduli, 3-12 GPa.

The sonic modulus and thermal expansivity are both closely related to the elastic properties of the molecules. The thermal expansivity parallel to the chain axis (a_2) is negative for many polymers. Thermal vibration leads however to thermal expansion in the perpendicular directions (α_1). The optical properties belong to a different group. The refractive index (tensor) is related to the polarizability (tensor) according to the Lorentz-Lorenz equation (Eq. (7.8)). In one group of polymers, polarizability is larger in the chain axis than in the transverse direction. This leads to a polymer with an intrinsic birefringence (Δn_0) greater than zero. The other group of polymers has strongly polarizable pendant groups and a negative intrinsic birefringence. It is difficult to make direct measurement of perfectly aligned samples. Highly oriented samples are measured and a low limit of Δn_0 can be obtained. In some cases, it is possible to determine the Hermans orientation function independently and, from a measurement of the in-plane birefringence of this particular sample, Δn_0 can be calculated according to Eq. (7.19). Theoretical calculation based on polarizability data is another possible method.

What is the relationship between degree of orientation and a given property? The answer obviously depends on what property is asked for and also what polymer is considered.

Let us discuss in more detail the elastic properties of highly (ultra) oriented polymers. It is known that the elastic modulus shows a good correlation with the draw ratio. For a given polymer, this relationship is fairly unique. The correlation between elastic modulus and the Hermans orientation functions f, f_c or f_a is not unique in that sense. It may be argued on the basis of the data of Sadler and Barham (1990) that the relevant correlation is between Young's modulus and molecular draw ratio (Fig. 7.21). A high **c**-axis orientation is achieved already at relatively low draw ratios and it increases only moderately on further drawing. The molecular draw ratio assesses the extension of the end-to-end vectors and the axial molecular continuity of the microfibrils. It is believed that long and thin molecular connections, amorphous or crystalline, constitute a ‘third’ strongly reinforcing component in the oriented semicrystalline polymer.

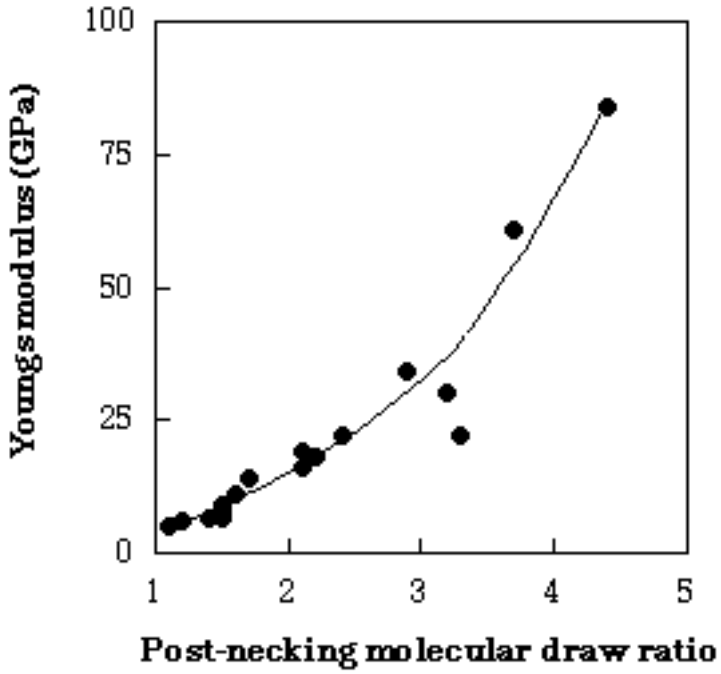

Fig. 7.21. Young's modulus of cold-drawn polyethylene as a function of the post-necking molecular draw ratio. The molecular draw ratio precisely after necking is close to 8. Drawn after data from Sadler and Barham (1990).

7.7. Summary

Chain orientation arises from the uni-dimensional character of polymers. Most properties are directional dependent with respect to the polymer chain. The origin of this intrinsic anisotropy lies in the presence of two different types of bonds, namely the covalent bonds and the family of weak, secondary bonds. Polarizability also shows a very strong directional dependence. The elastic modulus of polymers is always highest parallel to the chain axis. Polymers with a fully extended (all-trans) conformation show room temperature (intrinsic) values between 150 and 350 GPa. The modulus of polymers with a helical conformation is only about 50 GPa. The transverse moduli, which are controlled by the secondary bonds, are equal to only a few to ten GPa. The directional dependence of the polarizability leads to birefringence. The intrinsic (maximum) birefringence can, when strong polarizable groups are present in the backbone chain, amount to 0.2-0.3.

Chain orientation is a purely geometrical quantity of a system. If the polymer segments have a preferential direction, the system is said to be oriented. The ‘system’ can be a whole specimen, a small part of that specimen, the crystalline component of the specimen, the amorphous component of the specimen, etc. The preferential direction is called the "director" and the angle between the chain segments and the director is

denoted *f*. Hermans orientation function (*f*), the most frequently used quantity for the characterization of uniaxial orientation, is defined as follows:

$$f = \frac{3\langle \cos^2 \phi \rangle - 1}{2} \tag{7.47}$$

P. H. Hermans showed in the 1940´s that the in-plane birefringence ($\Delta n = n_3 - n_1 = n_3 - n_2$) where '3' denotes the director) is proportional to the orientation function:

$$\Delta n = \Delta n_0 f \tag{7.48}$$

where Δn_0 is the maximum (intrinsic) birefringence. The Hermans orientation function takes the value 1 for a system with perfect orientation parallel to the director and it takes the value -1/2 for the very same sample but with the director perpendicular to the chain axis. The Hermans orientation function is zero for an unoriented sample. Liquid crystalline polymers are often characterized by their order parameter (denoted S). This quantity is equivalent to the Hermans orientation function.

The orientation can be viewed in more general terms by an orientation probability function $f(\phi)$. It is implicit in this statement that the orientation in the plane perpendicular to the director is random, i.e. orientation is uniaxial. It is possibly to represent $f(\phi)$ by a series of spherical harmonics (Fourier series):

$$f(\phi) = \sum_{n=0}^{\infty} \left(n + \frac{1}{2} \right) \langle f_n \rangle f_n(\phi) \tag{7.49}$$

where the odd components are all zero and the first three even components are given by:

$$f_2(\phi) = \frac{1}{2}\left(3\cos^2 \phi - 1\right) \tag{7.50}$$

$$f_4(\phi) = \frac{1}{8}\left(35\cos^4 \phi - 30\cos^2 \phi + 3\right) \tag{7.51}$$

$$f_6(\phi) = \frac{1}{6}\left(231\cos^6 \phi - 15\cos^4 \phi + 105\cos^2 \phi - 5\right) \tag{7.52}$$

The parameters $\langle f_n \rangle$ are the average values. Note that f_2 is the Hermans orientation function. The full description of uniaxial orientation $f(\phi)$ can thus not be given by a single measurement of birefringence. Polymers may also show biaxial orientation. The segmental orientation function is in this case a function of two angular variables, i.e.

f(ϕ,υ). Assessment of biaxial orientation can be assessed by optical methods measuring the in-plane birefringence in the three orthogonal directions:

$$n_3 - n_1 = \Delta n_0 \left(f - \frac{g}{2} \right) \tag{7.53}$$

$$n_3 - n_2 = \Delta n_0 \left(f + \frac{g}{2} \right) \tag{7.54}$$

$$n_1 - n_2 = \Delta n_0 g \tag{7.55}$$

where $f = \frac{1}{2}\left(3\left\langle \cos^2 \phi \right\rangle - 1\right)$ and $g = \left\langle \sin^2 \phi \cdot \cos 2\upsilon \right\rangle$

Chain (segmental) orientation can be determined by a number of methods, e.g. optical methods measuring birefringence, wide-angle X-ray diffraction (crystalline orientation), infrared spectroscopy and measurement of sonic modulus. Determination of birefringence and sonic modulus provides only data yielding the Hermans orientation function whereas the X-ray diffraction method provides information about the full orientation function (f(ϕ) or f(ϕ,υ)). Neutron scattering only more recently assessed the orientation of the end-to-end vector.

Orientation is the result of deformation. "Mobile" molecules are extended by the application of an external force field (mechanical, electric or magnetic). The oriented state is frozen-in by "quenching" of the sample, e.g. by rapid cooling or by a pressure increase. The methods by which chain orientation is obtained may be divided into solid-state and liquid-state processes. The solid-state processes, i.e. cold-drawing, extrusion or rolling involve a plastic deformation of an isotropic or weakly anisotropic solid. The polymers that can be substantially oriented are semi-crystalline with deformable amorphous and crystalline phases. Cold-drawing/solid-state extrusion of a semi-crystalline polymer involves initially the deformation of the spherulitic structure, the subsequent transformation of the spherulitic structure to a fibrillar structure and finally the plastic deformation of the fibrillar structure. A polymer can only be cold-drawn or solid-state extruded to an ultra-oriented fibre if the following conditions are fulfilled: (a) a crystalline α relaxation must be present; (b) chain entanglements must be largely absent; (c) the number of interlamellar tie chains must be sufficiently high to prevent early brittle fracture.

The liquid-processes include melt-spinning and solution-spinning of crystalline or liquid-crystalline polymers. The melt or the solution is strained and the molecules are stretched from their equilibrium isotropic Gaussian states (flexible-chains) or simply aligned with the flow field (rigid rods). It is important that the oriented liquid-like state is rapidly transformed to the solid-state with a minimum of relaxation. This is more readily achieved with high molar mass polymers. The oriented liquid may be

"quenched" by a rapid elevation of the hydrostatic pressure or by rapid cooling producing an "interlocked shish-kebab" morphology in the case of polyethylene.

Most properties are strongly influenced by chain orientation. Birefringence, thermal expansivity, thermal conductivity and the elastic modulus depend on the Hermans orientation function according to relatively simple formulae. However, the elastic modulus of ultra-oriented polymers depends more directly on the macroscopic and molecular draw ratio. The latter reflects the extension of the end-to-end vector and the axial chain continuity.

7.8. Exercises

7.1. Calculate the chain orientation (Hermans orientation function) of the following schematic molecules:

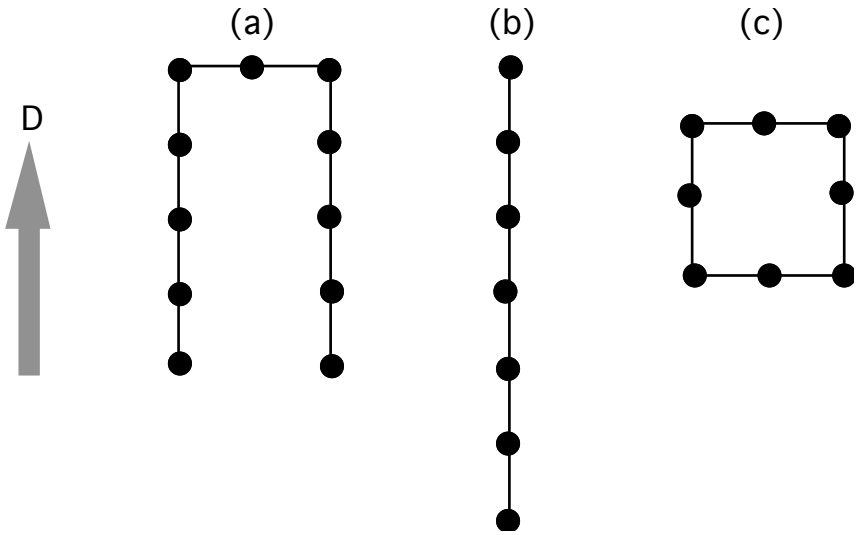

Fig. 7.22. Three molecules oriented differently in the plane with a common director (D)

7.2. The maximum birefringence ($\Delta n_0 = n_c - n_t$, where n_c is the refractive along the chain axis and n_t is the refractive index in the transverse direction) of the following polymers is:

Polymer	Δn_0
Poly(ethylene terephthalate)	0.25
Polycarbonate	0.24
Poly(vinyl chloride)	0.01
Polystyrene	-0.16

Source: Struik (1990).

Discuss the molecular reasons for the large differences in Δn_0 among the different polymers.

7.3. Calculate the crystalline chain orientation from the azimuthal-angle-dependence of the (hk0) X-ray reflection:

f (degrees)	0	20	60	65	70	75	80	85	90
I	0	0	0	2	4	8	16	40	60

Note that the director is set parallel to the average chain axis direction.

7.4. Calculate the amorphous chain axis orientation for the same polymer sample. The overall chain orientation was determined by optical methods to be 0.8. The crystallinity was determined by DSC to be 50%.

7.5. Draw schematic X-ray diffraction patterns of (00l) in a sample with uniaxial orientation along the z-axis in the **xz**-, **yz**- and **xy**-planes.

7.6. Draw the same X-ray diffraction patterns for a sample showing biaxial orientation.

7.7. Draw schematically the infrared absorbance at 1700 cm^{-1} (carbonyl stretching band) as a function of the angle (f) between the polarization direction of the infrared light and the fibre axis of a polyester fibre. Indicate also how the chain axis orientation can be obtained from the IR absorbance data.

7.8. Define molecular draw ratio. How can it be measured?

7.9. Why is it impossible to extrude PA6 through a very narrow die at temperatures well below the melting point? Why is the same action possible in the case of polyethylene?

7.9. References

Bettelheim FA, Stein RS (1958) J Polym Sci 27:567.

Folkes MJ, Keller A. (1971) Polymer 12:222.

Gedde UW, Andersson A, Hellermark C, Jonsson H, Sahlén F, Hult A. (1993) Progr Coll Polym Sci 92:129.

Hay IL. (1980) 'Production and measurement of orientation', in 'Methods of experimental physics', Vol. 16, Part C (R. A. Fava, ed.) Academic Press, New York, p. 137-184.

Hedmark PG, Rego Lopez JM, Westdahl M, Werner P-E, Gedde, UW. (1988) Polym Eng Sci 28:1248.

Holliday L, White J.W. (1971) Pure Appl Chemistry 26:245.

Mackley MR, Keller A. (1973) Polymer 14:16.

Peterlin A. (1979) Mechanical properties of fibrous polymers, in Ultrahigh Modulus Polymers (A. Ciferri and I. M. Ward, eds.), p. 279. Applied Science Publishers, London.
Read BE, Duncan JC, Meyer DE. (1984) Polymer Testing 4:143.
Sadler DM, Barham PJ. (1990) Polymer 31:46.
Samuels RJ. (1974) 'Structured polymer properties: the identification, interpretation and application of crystalline polymer structure', Wiley, New York.
Struik LCE. (1990) "Internal stresses, dimensional instabilities and molecular orientation in plastics", Wiley, Chichester and New York.
Young RJ. (1988) Materials Forum, 210.
Ward IM., ed. (1975) 'Structure and properties of oriented polymers', Applied Science Publishers, London.
Zachariades AE, Mead WT, Porter RS. (1979) Recent developments in ultramoleculara orientation of polyethylene by solid state extrusion, in Ultrahigh Modulus Polymers (A. Ciferri and I. M. Ward, eds.), p. 77. Applied Science Publishers, London.